

contexts ranging from cell dry mass measurements to measuring intracellular transport [9,32]. As shown in Fig. 1, SLIM is designed as an add-on module to a commercial phase contrast microscope (Zeiss Axio Observer Z1). For conventional phase contrast microscopy, a phase ring in the back focal plane of the objective is used to impart a $\pi/2$ phase shift to the un-scattered light, relative to the scattered light. For SLIM, the back focal plane of the phase contrast objective is projected onto a liquid crystal phase modulator which is used to impart additional phase shifts to the un-scattered light in increments of $\pi/2$. In total 4 intensity images are recorded corresponding to phase differences of $0, \pi/2, \pi$ and $3\pi/2$. A quantitative phase map may then be uniquely determined from these 4 images as previously described [26,27]. To ensure that the phase measured is integrated over the entire thickness of the cell we used a low numerical aperture (NA) objective. Thus, for both the SLIM and absorption measurements a 10x/0.3 Ph1 objective was used. The exposure time for each of the intensity maps is 15 milliseconds and a total of 0.75 second is required to acquire the 4 maps.

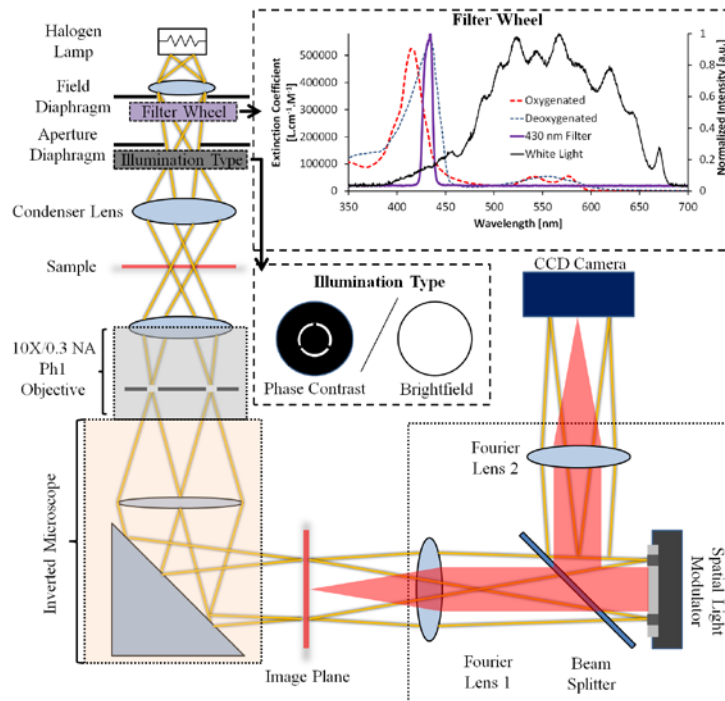


Fig. 1. Experimental setup. The SLIM system is built as an add-on module to a commercial phase contrast microscope. The back focal plane of the objective is projected onto a spatial light modulator which is calibrated to impart a phase shift to the un-scattered light (yellow lines) relative to the scattered light (shown in red). Four intensity images are recorded corresponding to 4 phase shifts in increments of $\pi/2$, the quantitative phase map is reconstructed from these 4 intensity images as detailed in Ref. [26]. For the SLIM measurements the illumination type is set to phase contrast and the filter wheel is set to an open position such that the entire spectrum of the halogen lamp is passed. For the absorption measurements the illumination type is set to bright field and a 430 nm filter is used in the filter wheel. The inset for the filter wheel shows the normalized intensity of the white light spectrum, the spectrum of the 430 nm bandpass filter (right axis) and the extinction coefficients of oxygenated and deoxygenated hemoglobin (left axis) as a function of wavelength from Ref. [33].

For measuring the absorption map a bandpass filter centered at 430 nm (± 10 nm) is introduced into the light path after the condenser field diaphragm as shown in Fig. 1. In principle any bandpass filter could be used, provided the SNR is high enough. The choice of 430 nm was made since it is strongly absorbed by both oxygenated and deoxygenated hemoglobin. The phase contrast annulus in the condenser is also swung out of position so

that the illumination is set for bright-field measurements. In order to optimize the absorption measurement, both the NA of the condenser and the objective must be taken into account. As for the SLIM measurement the NA of the objective must be chosen such that the depth of field is greater than the thickness of the red blood cells. The optimal NA for the condenser was determined experimentally by varying NA between 0.55 and 0.1 and measuring the absorption. It was found for multiple objectives (data not shown) that the absorption continues to increase as the NA is decreased and peaks at a value close to the NA of the objective being used. After this point, aberrations become clearly observable in the image. For the 10x/0.3 objective used here, the value for the condenser NA which gave the greatest contrast was determined to be 0.2. For the absorption measurements an exposure time of 250 milliseconds is used. For each patient a 1.55 x 1.01 mm area is scanned corresponding to a 4x4 mosaic. When taking into account the time required for moving the stage and switching from SLIM to brightfield it takes approximately 2 minutes to measure each patient.

Although in principle any QPI technique could be coupled with an absorption measurement to yield results similar to those shown here, we used SLIM for two main reasons. First, the white light illumination used for SLIM allows for easy integration of a filter wheel into the setup to perform absorption measurements. Second, SLIM provides the lowest noise and highest sensitivities out of any QPI technique that we are aware of.

3.2. Data analysis

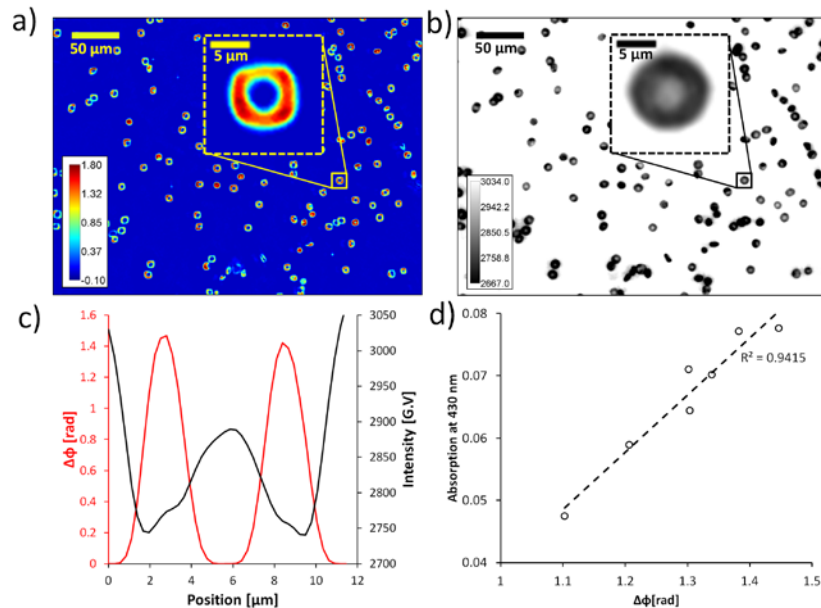


Fig. 2. Image analysis (a) Quantitative phase map acquired using SLIM, color bar is in radians. (b) Absorption map acquired at 430 nm, color bar is in 16-bit gray scale values. (a-b) Insets show an example of a single RBC from the maps. (c) Overlay of 1 line profiles drawn through the center of a single cell, the phase values are shown in red against the left axis and the corresponding intensity from the absorption maps are shown in black against the right axis. (d) Average absorption vs. phase for each of the 7 patients analyzed in this study, a strong linear relationship (dotted line) indicates the feasibility of this method. For the cell shown here the volume and hemoglobin concentration were calculated to be 86.18 fL and 0.3 g/mL respectively.

To analyze the images, a semi-automatic image routine was developed in MATLAB. A user selects several cells in every image, avoiding cells that are turned on their side or appear otherwise damaged. Using this routine it takes approximately 5 minutes to analyze the data from one patient. Once a cell is picked the region occupied by the cell is identified by

generating a binary mask and the center of mass of this mask corresponds to the center of the cell. As can be seen in the inset to Fig. 2a the red blood cell appears to be less circular than expected, this is due to the square aperture of the spatial light modulator (SLM) which is not large enough to allow all the high frequency components when a small numerical aperture objective is used. This problem can be overcome by adjusting the magnification of the SLIM system, using a higher NA objective or using a larger aperture SLM. For each cell a horizontal and vertical line profile are then measured through the center, for both the absorption and phase map (Fig. 2c). This approach assumes that the cells are radially symmetric, which is a reasonable approximation for red blood cells, although for future clinical work a pixel by pixel comparison will be ideal. From the phase profiles the peak values are chosen and from the intensity profile the minima are chosen. As can be seen in Fig. 2c, the phase and absorption profiles are in good agreement except for in the dimple region of the blood cell. For this reason, to demonstrate the feasibility of this technique just the peak values were chosen for the analysis presented here. Of course, for clinical translation, this mismatch must be understood and addressed. Figure 2d shows that the phase and absorption measurements are in fact linearly related and proves the feasibility of this approach.

The peak values from the horizontal and vertical profiles are averaged and plugged into Eq. (5) and Eq. (6) to calculate the un-calibrated concentration and thickness values. For this analysis it is assumed that the blood cells are oxygenated and we obtained the absorption spectrum for hemoglobin from Ref. [33]. The volume for each cell is calculated by multiplying the average thickness, calculated from the line profiles, by the projected area of the cell. For calibration, the measured mean cell volume (MCV) and mean cell hemoglobin concentration (MCHC) values are plotted against the values reported by the CBC and a best fit line is calculate to provide a calibration function. In principle this analysis could be completely automated as previously shown [10,21], but is not necessary for the proof of principle of this technology.

4. Results

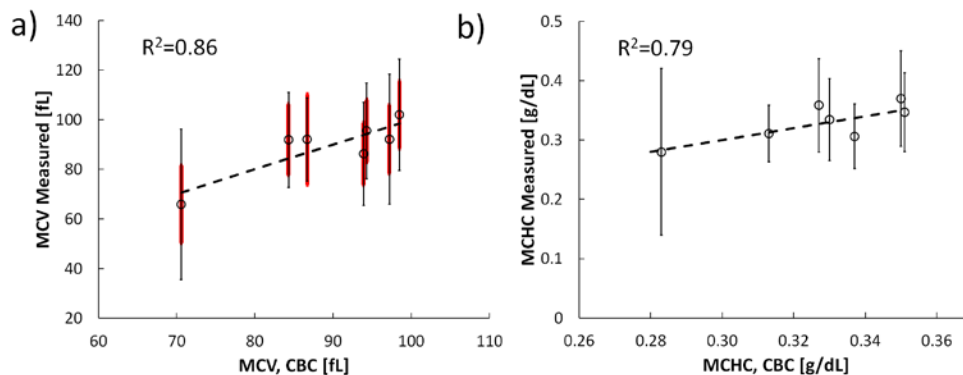


Fig. 3. Comparison of measured mean values with clinically reported values. (a) Mean Cell Volume, red error bars correspond to the SD reported by the Clinic and black error bars correspond to SD measured by the QPI and absorption measurements (b) Mean Cell Hemoglobin Concentration, error bars correspond to the measured SD, no SD information on the hemoglobin concentration is available from the Clinic. The dashed black lines have a slope of one.

For this study, samples from a total of 7 patients were measured and total of 651 cells were analyzed with an average of 93 cells per patient. The comparison between the calibrated mean values from our measurements and the CBC values is shown in Fig. 3. It can be seen that both the measured MCV and MCHC agree well, with R^2 values of 0.86 and 0.79, respectively. The discrepancies are likely due to two major reasons. First, the MCHC reported by the clinic is

calculated by lysing all the blood cells to make a solution of hemoglobin. An absorption measurement is then made on this solution to calculate the hemoglobin concentration.

Therefore, this measurement doesn't take into account any variability in hemoglobin concentration between cells. Secondly, the number of cells measured in this study is relatively low compared to the large numbers measured by the clinical impedance counters. Since the comparison between our measurements and the clinic relies on calibration, the agreement will likely increase with an increase in throughput.

For the volume measurement, Fig. 3a also shows the standard deviations measured by the clinic in red and those measured by our technique in black. The lack of perfect agreement in the distribution widths is most likely due to the higher sensitivity of our method and the difference in the sample sizes measured. Although the clinical counter we are comparing our measurement to, does provide a histogram of size distributions for each patient, it does not have the capability to do the same for hemoglobin concentration, Fig. 3b thus only shows the standard deviations in the hemoglobin concentration distributions measured by our technique. The fact that the clinical analyzer in a major community hospital does not have this capability illustrates the need for a simple approach to provide this measurement.

5. Discussion and conclusions

In this study we have shown both theoretically and experimentally that by combining quantitative phase measurements with bright field absorption measurements it is possible to calculate both cell morphology and hemoglobin concentration at a single cell level. The method was validated by comparing the values measured with those reported by a state of the art automated clinical blood analyzer. Although in this study a calibration was necessary, in the future a more detailed understanding of the formation of the bright field image may render this step unnecessary. In particular, the measured intensity includes contributions from scattered light and is not a pure absorption map as described by Beer's law. Furthermore Lambert-Beer's law must be rewritten for the case of convergent illumination as is provided by a typical microscope. The fact that the phase and absorption are linearly related, without taking these effects into account, indicates that the contribution from them is constant for red blood cells.

Although we used SLIM to measure phase, in principle this technology could be utilized in combination with any QPI method. However, SLIM is well suited for this method since it does not require any modifications to a commercial microscope and the filter wheel required for the absorption measurements may easily be integrated with the white light illumination. The fact that SLIM requires 4 intensity measurements is only a practical issue as the advent of fast spatial light modulators, cameras and scanning software means that the speed of the measurement may easily be increased. Furthermore, the high SNR provided by SLIM ensures that data analysis technology can easily be automated to increase throughput. Since SLIM can simply be added as a modality to an existing microscope, minimal re-training will be necessary to use the equipment especially given that the parameters provided by this analysis are already familiar to pathologists and technicians.

In conclusion, the technology presented here offers a powerful new blood screening tool that may aid pathologists in making differential diagnosis and risk stratification. This technology combined with the morphological analysis described previously [10,21] provides the ability to analyze red blood cells with unprecedented details and may enable new diagnostic capabilities when monitoring and treating red blood cell disorders. Furthermore, the ability to easily measure single cell hemoglobin concentrations may open new avenues for monitoring blood cell disorders and the effects of treatment.

Acknowledgments

This research was supported in part by the National Cancer Institute (R21 CA147967-01) and the National Science Foundation (grants CBET 08-46660 CAREER, CBET-1040462 MRI, CBET-0939511). For more information, visit <http://light.ece.uiuc.edu/>.